Risk Assessment of Offshore Wind Farm Outages Under Typhoon Conditions

Yanqi Liu, Hongxun Hui, *IEEE Member*, Hongcai Zhang, *IEEE Member*, Liang Gao

State Key Laboratory of Internet of Things for Smart City, University of Macau, Macao, China
(hczhang@um.edu.mo)

2022 IEEE Power & Energy Society General Meeting (PESGM) | 978-1-6654-0823-3/22/$31.00 ©2022 IEEE | DOI: 10.1109/PESGM48719.2022.9916685

***Abstract*—The offshore wind energy is increasing rapidly due to higher stability and efficiency than onshore one. However, offshore wind farms suffer from typhoon activities, which cause unpredictable outages and threaten the system secure operation. Previously, few studies consider the operating risk of offshore wind farm under typhoon conditions. To bridge this gap, this paper assesses the risk of offshore wind farm outages facing typhoon disasters. First, based on a data-driven method, typhoon tracks are simulated using empirical formulas considering uncertainties. Then the typhoon influence on offshore wind farms is analyzed to obtain the dynamic power generation. Finally, the dispatchable region is enveloped to identify power system risk states. On this basis, the resilience indices are calculated for the system secure operation. Numerical experiments are carried out to validate the proposed models and methods. The simulation results show that the operation risks of the power system can be effectively assessed under typhoon conditions.**

Keywords*—*typhoon disaster, offshore wind farm, risk assessment, uncertain track.

I. Introduction

The offshore wind energy is increasing rapidly due to higher stability and efficiency than onshore one [1]. For example, the installed capacity of offshore wind power has increased to 40GW around the world [2]. However, offshore wind farms are susceptible to extreme weather events such as typhoons [3], which is also this paper focuses on. Typhoons can cause wind farm outages and bring power imbalance, which threaten the power system's voltage and frequency security [4].

To address this issue, Yang et al. [5] propose a new quantitative resilience assessment index for power transmission systems considering the duration and disruption features of typhoons. Sang et al. [6] study the transmission tower structural model and propose an integrated preventive framework considering weather forecast to reduce typhoon damages. However, these papers mainly focus on resilience assessment of the power transmission system, including transmission lines, towers and substations, while not the influence on offshore wind farms. Actually, offshore wind farms stand in the breach of typhoon and are most likely to shut down because of the high wind speed. When the reserve is inadequate to cover the wind power gap, there is a severe active power imbalance between the supply- and demand-side, causing the power system insecurity and instability [7]. Thus, it is critical to assess the power system operation risks arising from offshore wind farm outages.

The operation states of offshore wind farms are directly impacted by the weather conditions. Many papers reveal the typhoon influence considering failure mechanism of power system components. For example, the deterministic typhoon track model is used for the reliability and damage assessment in [8]. Specific typhoon tracks and time-varying impacts are utilized to achieve grid hardening strategy against typhoons in [9]. A probabilistic line failure model is used to construct the line failure ambiguity set in [10], while the uncertainty of hurricane track is not revealed. Therefore, this paper simulates typhoon tracks using empirical formulas considering uncertainties based on a data-driven method. Then the typhoon influence on offshore wind farms is analyzed to obtain the dynamic power generation. Finally, the dispatchable region is enveloped to identify power system risk states [11]. On this basis, the resilience indices are calculated for the system secure operation. Numerical experiments are carried out to validate the proposed models and methods. The simulation results show that the operation risks of the power system can be effectively assessed under typhoon conditions. To sum up, this paper uses a data-driven method to generate typhoon track scenarios and assesses the operating risks identified by the dispatchable region during typhoon landings.

The rest of this paper is organized as follows. Section II and III introduces the typhoon model and offshore wind farm model respectively. Section IV presents the dispatchable region and risk indices in power system assessment and Section V provides the numerical experiments. Conclusions are drawn in Section VI.

II. Modeling of Typhoon Conditions

In this section, the spatial temporal characteristics of typhoons are first introduced to study the typhoon impacts on offshore wind farms. Considering typhoon affects offshore wind farms with intense wind force, a typhoon center track model is formulated based on the empirical formulas. In the day ahead forecast, the typhoon track prediction is not very accurate. Thus we use a statistical method to obtain the track uncertainties.

A. Modeling of typhoon forecast track

The typhoon track model includes the typhoon translation model and typhoon central pressure model. An empirical track model is developed in [12] to describe the typhoon translational wind speed and heading direction, as follows:

$$\begin{aligned}\Delta \ln c = a_1(t) + a_2(t)\psi(t) + a_3\lambda(t) + \\ a_4(t)\ln c(t) + a_5(t)\theta(t) + \varepsilon_c\end{aligned}, \tag{1}$$

$$\begin{aligned}\Delta \theta = b_1(t) + b_2(t)\psi(t) + b_3\lambda(t) + b_4(t)c(t) + \\ b_5(t)\theta(t) + b_6(t)\theta(t-\Delta t) + \varepsilon_\theta\end{aligned}, \tag{2}$$

where c represents the translational wind speed; θ is the heading angle; $\Delta\ln c = \ln c(t+\Delta t) - \ln c(t)$; $\Delta\ln\theta = \ln\theta(t+\Delta t) - \ln\theta(t)$; Δt is the time step length; ψ and λ denote the typhoon latitude and longitude, respectively. The residual terms ε_c and ε_θ are assumed to follow the normal distribution with the mean value equal to zero. The interested typhoon active area is divided into 5°×5° grids. Each grid has its own parameters to model the typhoon location in the next time step. The parameters $a_1(t) \sim a_5(t)$ and $b_1(t) \sim b_5(t)$ are model coefficients

XXX-X-XXXX-XXXX-X/XX/$XX.00 ©20XX IEEE
978-1-6654-0823-3/22/$31.00 ©2022 IEEE

for each region calculated from historical data through linear regression.

The typhoon relative intensity model can be used to calculate the central pressure and gradient wind field. The relative intensity is related to sea surface temperature [8]:

$$\begin{aligned}\ln I(t+\Delta t) &= d_1(t) + d_2(t)\ln I(t) + d_3 \ln I(t-\Delta t) + d_4(t) \\ \ln I(t-2\Delta t) &+ d_5(t)T_s(t) + d_6(t)(T_s(t+\Delta t) - T_s(t)) + \varepsilon_I,\end{aligned} \quad (3)$$

where T_s(t) is the sea surface temperature; $d_1(t)$ to $d_6(t)$ are model coefficients derived from the above 5°×5° grids. The e_I is the residual terms. In the simulation process, the historical typhoon data is collected in time interval of 6 hours by Tropical Cyclone Center of China Meteorological Administration [13].

B. Modeling of typhoon track uncertainties

In last subsection, a simulated typhoon track is presented. However, it remains forecast errors which will accumulate over time. The historical data are exploited to obtain the forecast error and model the track uncertainty. The probability distribution of the forecast track error is obtained in the following steps. Here we take six hours forecast error for example, as shown in Fig. 1.

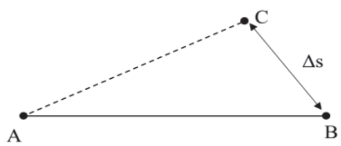

Fig. 1. Typhoon track forecast error

1) Input the locations of two adjacent historical point (e.g. A and B) from typhoon track data.
2) Use empirical formula to calculate forecast location C in the next time interval based on A.
3) Obtain the distance of A and C as the track forecast error.
4) Input typhoon historical track and obtain a series of forecast errors in the six hours.
5) The probability density function (PDF) is deduced by kernel function estimation.

C. Modeling of typhoon wind field

The typhoon wind field is portrayed as a vortex and the field contour lines are concentric circles [14]. At each time snapshot, the static wind field of a typhoon can be determined as a function of the distance to the typhoon center (eye):

$$w_t = \begin{cases} Kw_m[1-\exp(-\alpha x)], 0 \le x \le r_{mw} \\ w_m \exp[-\ln\beta * (x - r_{mw})/(r_s - r_{ms})], r_{mw} \le x \le r_s \\ 0, r_s < x \end{cases} \quad (4)$$

where

$$\alpha = \frac{1}{r_{mw}} \ln(\frac{Q}{Q-1}) . \quad (5)$$

The Q reflects the typhoon boundary and K is typhoon speed parameter; W_m is the maximum wind speed at about 10m above the surface and r_{mw} is the distance from typhoon eye correspond to the maximum wind speed. The typhoon boundary (r_s) is assumed to be a circle where the typhoon wind speed has reduced to W_m/β. The area that lies outside the typhoon boundary will not be impacted by the typhoon. Symbol x denotes the distance from the typhoon eye to the offshore wind farms. In this paper, the parameters K and Q are set to 1.14 and 10, respectively. Accordingly, the wind speed is depended on time-varying parameters W_m, r_{mw} and r_s given the typhoon center location.

In order to estimate the parameters W_m, r_{mw} and r_s, this paper adopts the model in [15], as follows:

$$\ln r_{mw} = 2.636 - 0.0005086\Delta p^2 + 0.0394899\psi , \quad (6)$$

$$w_m = \sqrt{B\Delta p / e\rho} , \quad (7)$$

$$B = 1.38 + 0.00184\Delta p - 0.00309 R_{\max} . \quad (8)$$

In (6), the central pressure difference (Δp) is calculated from relative intensity $I(t)$ in (3), the relationship of two parameters can be described as [16]:

$$I(t) = \frac{\Delta p}{p_{da} - p_{dc}} , \quad (9)$$

where p_{da} represents the surface value of the partial pressure of ambient dry air; p_{dc} denotes the minimum sustainable surface value of central pressure for a typhoon.

III. Modeling of Offshore Wind Farms

A. Typhoon wind speed at the offshore wind farm sites

During typhoon crossing period, the offshore wind farms are affected by storm wind. When the typhoon center location with a probability information is given, the wind speed at each offshore wind farm site depends on the distance from the typhoon center, as follows:

$$d = ((x_w - x(t))^2 + (y_w - y(t))^2)^{0.5} , \quad (10)$$

where ($x(t)$, $y(t)$) and ($x_w(t)$, $y_w(t)$) are the location of the typhoon center and the offshore wind farms, respectively; d is the distance between them.

B. The output power of the offshore wind farm

The wind turbines only operate if the wind speed is between the cut-in speed and cut-off speed. The output power of the wind farm is as follows:

$$p_{out} = \begin{cases} 0, \quad w \le w_{ci} \text{ or } w \ge w_{co} \\ P_r \dfrac{w - w_{ci}}{w_r - w_{ci}}, \quad w_{ci} < w \le w_r \\ P_r, \quad w_r < w < w_{co} \end{cases} , \quad (11)$$

where P_{out} is output power of the offshore wind farm; w_{ci} and w_{co} are the cut-in wind speed and cut-out wind speed, respectively; v_{r} is the rated wind speed; P_{r} is the rated output of the offshore wind farm. In this paper, the cut-in, cut-out and rated wind speeds are set to 3, 12 and 20 m/s, respectively.

IV. Offshore Wind Farm Outage Risk and Resilience Assessment Method

Based on the typhoon model and wind farm model in the last sections, this paper considers the simulated typhoon and track uncertainties to analyze its influence on the offshore wind farms. In this section, the system security states are assessed and resilience indices are proposed and calculated. The paper follows the classical reliability indices considering the probability of power unsafe states and expected power loss. We assume the offshore wind farms are affected by the typhoon activities and the wind power outputs deviating the

978-1-6654-0823-3/22/$31.00 ©2022 IEEE

forecast ones threatens the power balance in real time dispatch. Thus, the risk index R in a period time can be formulated as:

$$R = \sum\nolimits_{T} I_s \cdot \Delta p_T \,, \tag{12}$$

where I_s is the sign function representing the system security and Δp_T denotes wind power output deviations causing load loss at the T time slot. The dispatchable region [11] of a power system is defined as the largest range of a power injection that the power system can accommodate in a certain dispatch interval. Thus, the dispatchable region is utilized to identify the power system operating states in the following steps:

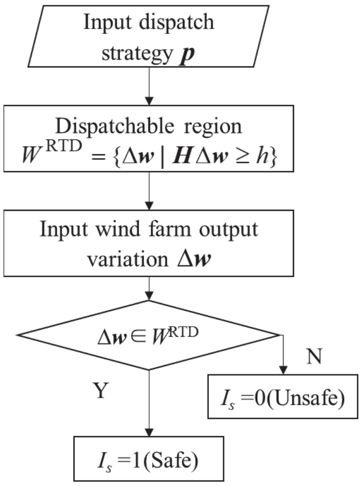

Fig. 2. The risk states identified by dispatchable region

The assessment process is illustrated in the following flow chart in Fig. 3.

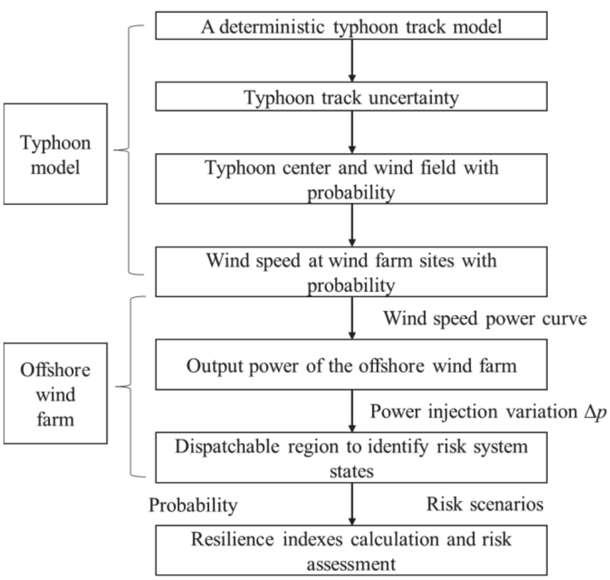

Fig. 3. The flow chart of the assessment process

1) Formulate the deterministic typhoon track. Obtain the initial conditions of typhoon (the observed typhoon location, relative intensity at that time) and simulate the deterministic typhoon track based on the empirical formula (1)-(3).

2) Calculate the typhoon track uncertainty. The track forecast errors in different time ahead are collected. The kernel density estimation is utilized to predict the forecast track error and probabilistic information.

3) Determine the typhoon center and wind speed at the offshore wind farm sites. The typhoon track uncertainty leads to variable wind speed at the offshore wind farm sites, which results in uncertain output power and different operational states.

4) Obtain the output deviation of offshore wind farms and calculate the dispatchable region. Identify the risk system state and calculate the risk index.

V. Case Studies

A modified IEEE 30-bus system with two offshore wind farms at buses #1 and #22 and a simulated typhoon are used to illustrate the proposed method. The topology of the test system is presented in Fig. 4. Two offshore wind farms are located at 25°N,120°E and 24.3°N,123°E, respectively. The capacity of these two wind farms are 40 MW and 60 MW, respectively. The daily maximum load demand is scaled up to 241.16 MW.

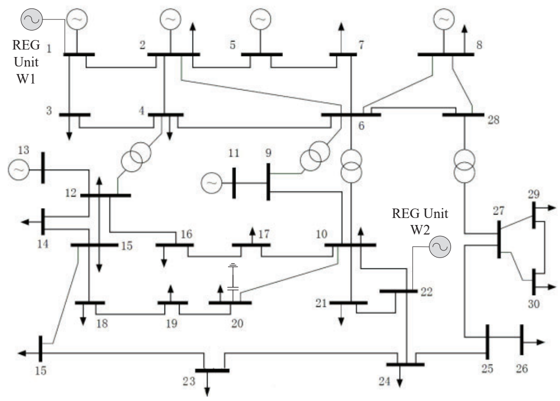

Fig. 4. The topology of the modified IEEE 30-bus system

A. Typhoon simulation

We assume the typhoon landing is located in China southeastern coast and the interested typhoon active area extends from 10°N to 25°N (northern latitude), 110°E to 130°E (east longitude), divided into 12 regions. The simulated typhoon is moving in the northwest direction in Fig. 5.

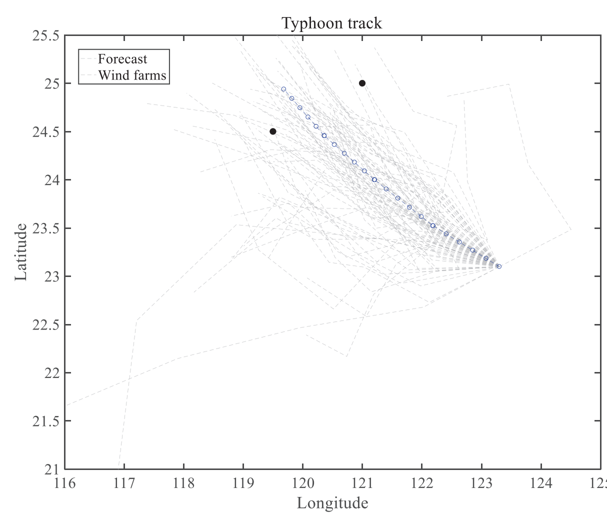

Fig. 5. Typhoon track and offshore wind farm sites

The blue solid line is the real track obtained from typhoon historical data and the blue dotted line is the forecast track simulated by the empirical formula (1)-(3). The light gray lines are the possible paths indicating the typhoon forecast errors and track uncertainty.

The typhoon forecast track errors affect the distance from typhoon center to wind farms, which leads to uncertain wind generation and unpredictable wind farms operating states. To reveal the typhoon track uncertainty, the forecast errors of the simulated typhoon track are collected in Section II-B. The kernel density estimate method is used to obtain the probability distribution information. The probability density distribution (PDF) and the cumulative distribution function (CDF) of the typhoon track forecast errors are shown in Fig. 6 and Fig. 7. It is found that regarding the typhoon track uncertainty (Case 3) figures out more precise wind farm output expectation while the forecast typhoon track (Case 2) fails to predict output deviation in wind farm 2 (W2).

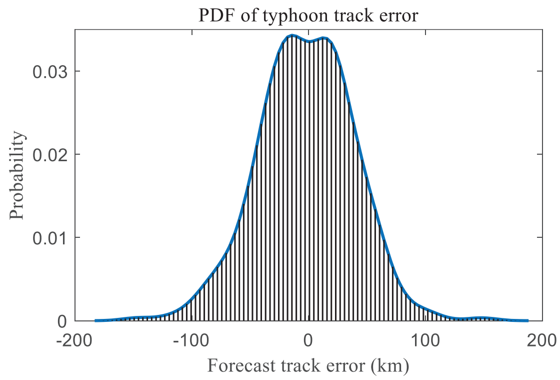

Fig. 6. PDF of typhoon track error

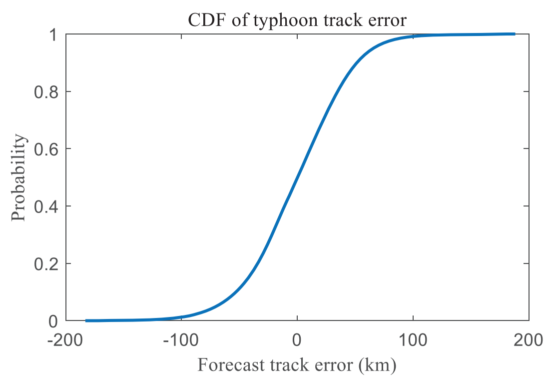

Fig. 7. CDF of typhoon track error

B. Risk assessment

During the typhoon activity, the offshore wind farms are influenced due to the violent wind speed. This paper assesses the power system operating risks with wind power deviation. Suppose the typhoon track is known in advance, system operators are supposed to carry out proper preventive dispatch strategy to minimize the load shedding and wind power loss. In this section, we analyze different day ahead unit commitment (UC) strategies, Case 1 and Case 2, and calculate their operating risks during the typhoon activities.

Case 1: The typhoon landing is ignored and day ahead unit commitment is calculated based on normal weather condition. The forecast outputs of two offshore wind farms are shown in Fig. 8 and the UC is presents in Fig. 9.

Case 2: The forecast outputs of the offshore wind farms are affected by the typhoon track is plotted in Fig. 10 and the corresponding UC is shown in Fig. 11.

Under actual circumstances with uncertainty, the power outputs are deviated from the forecast ones and the power imbalances threaten the real time dispatch. In every time interval, the output deviations, Δp_T, are input into dispatchable region to make sure the power system operating states are safe or not. I_s is determined by the dispatchable region in Fig. 12. The risk indices are calculated based on (12) in TABLE I.

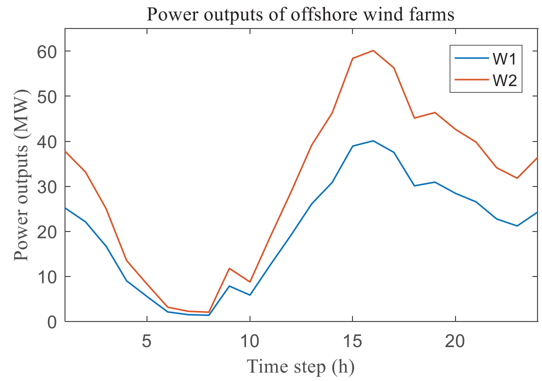

Fig. 8. Forecast outputs of two wind farms regardless of typhoon

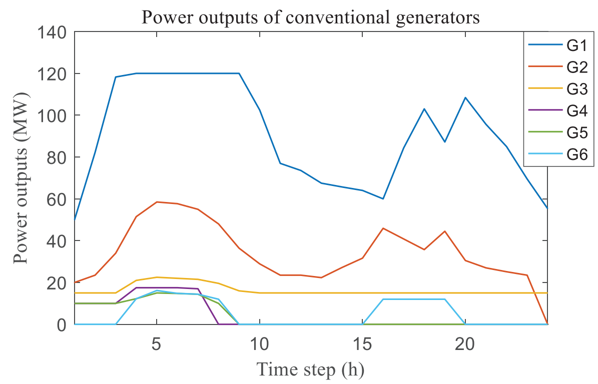

Fig. 9. Security constrained UC regardless of typhoon

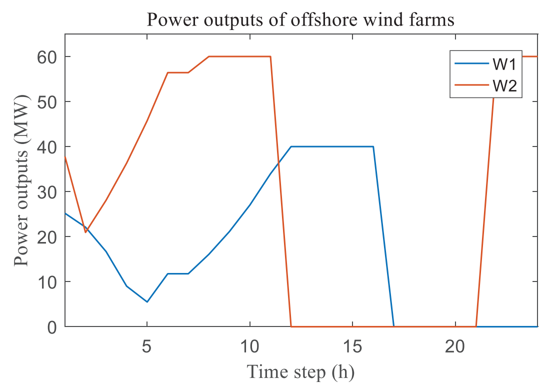

Fig. 10. Two wind farms under forecast typhoon track

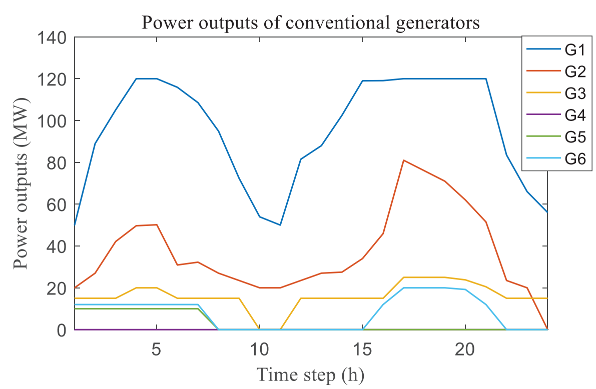

978-1-6654-0823-3/22/$31.00 ©2022 IEEE

Fig. 11. Security constrained UC under forecast typhoon track

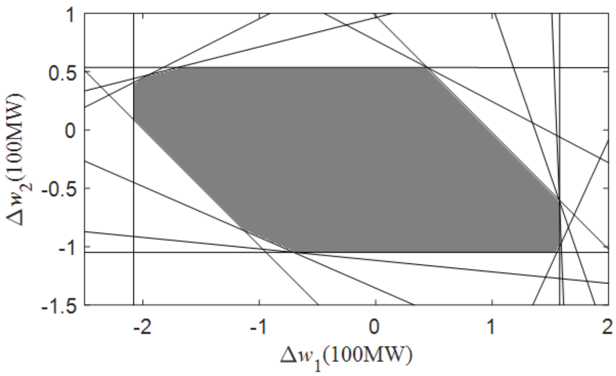

Fig. 12. The dispatchable region in 6th time slot

TABLE I
UNSAFE STATES AND RISK INDICES

Case	Unsafe states	Risk indices
Case 1	12	1.6045
Case 2	4	0.1124

In cases 1 and 2, the wind power outputs are outside the dispatchable region because of the large power imbalance. Compared to Case 1, Case 2 considers the simulated typhoon track and the forecast wind power outputs are more accurate resulting in smaller total risks and less unsafe states.

The unsafe states of Cases 1 and 2 are displayed in Fig. 13 and Fig. 14. The average risk in different time steps indicate the riskiest states are among 23 ~ 24 time intervals in both cases. However, regardless simulated typhoon can reduce the average risks and total unsafe states.

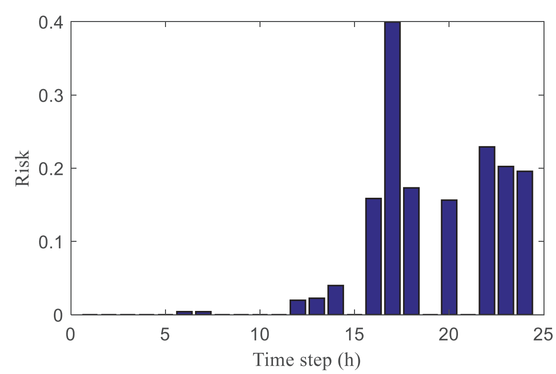

Fig. 13 The unsafe states regardless of typhoon

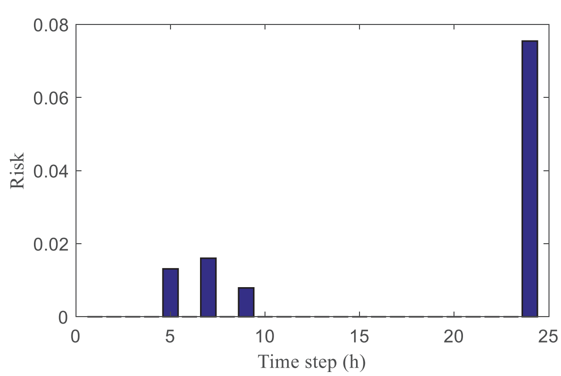

Fig. 14 The unsafe states regarding simulated typhoon

VI. CONCLUSIONS

The paper assesses the power system operating risks caused by offshore wind farm outages under typhoon conditions. A simulated typhoon with uncertain track is revealed to study the spatial temporal feature and its impact on offshore wind farms. The dispatchable region is utilized to assess the power system operating security. It is found the simulated typhoon with track uncertainty can better seek out the operating risks of offshore wind farms with probabilistic information. The proposed method can not only calculate the total operating risk during typhoon activities, but also identify the unsafe states in different time slots. Future work may focus on the unit commitment and anti-risk dispatch strategy.

VII. ACKNOWLEDGEMENT

This paper is funded in part by the Science and Technology Development Fund, Macau SAR (File no. SKL-IOTSC(UM)-2021-2023, and File no. 0137/2019/A3).

REFERENCES

[1] P. Sherman, X. Chen, and M. McElroy, “Offshore wind: An opportunity for cost-competitive decarbonization of China’s energy economy,” *Science Advances*, vol. 6, no. 8. 2020.

[2] L. Gao, G. Cai, Y. Zhang, S. Ke, and Y. Chen, “Study on the Economic Optimization of Energy Storage System Configuration for Wind Power Accommodation in Guangdong Province,” *IOP Conf. Ser. Earth Environ. Sci.*, vol. 555, no. 1, 2020.

[3] S. Yuan, S. M. Quiring, L. Zhu, Y. Huang, and J. Wang, “Development of a Typhoon Power Outage Model in Guangdong, China,” *Int. J. Electr. Power Energy Syst.*, vol. 117, no. June 2019.

[4] R. Fang, W. Yang, T. Huang, et al. "The Shutdown Risk Assessment of Wind Farms under Typhoon Disaster." *2020 IEEE 4th Conference on Energy Internet and Energy System Integration (EI2)*. 2020.

[5] Y. Yang, W. Tang, Y. Liu, Y. Xin, and Q. Wu, “Quantitative Resilience Assessment for Power Transmission Systems under Typhoon Weather,” *IEEE Access*, vol. 6, pp. 40747–40756, 2018.

[6] Y. Sang, J. Xue, M. Sahraei-Ardakani, and G. Ou, “An Integrated Preventive Operation Framework for Power Systems during Hurricanes,” *IEEE Syst. J.*, vol. 14, no. 3, pp. 3245–3255, 2020.

[7] Q. Wang, Z. Yu, R. Ye, Z. Lin, and Y. Tang, “An ordered curtailment strategy for offshore wind power under extreme weather conditions considering the resilience of the grid,” *IEEE Access*, vol. 7, no. April, pp. 54824–54833, 2019.

[8] H. Zhang, L. Cheng, S. Yao, T. Zhao, and P. Wang, “Spatial-Temporal Reliability and Damage Assessment of Transmission Networks under Hurricanes,” *IEEE Trans. Smart Grid*, vol. 11, no. 2, pp. 1044–1054, 2020.

[9] S. Ma, B. Chen, and Z. Wang, “Resilience Enhancement Strategy for Distribution Systems Under Extreme Weather Events Shanshan,” *IEEE Trans. Smart Grid*, vol. 9, no. 2, pp. 1442–1451, 2018.

[10] T. Zhao, H. Zhang, X. Liu, S. Yao, and P. Wang, “Resilient unit commitment for day-ahead market considering probabilistic impacts of hurricanes,” *arXiv*, vol. 8950, no. c, pp. 1–13, 2019.

[11] W. Wei, F. Liu, and S. Mei, “Real-time dispatchability of bulk power systems with volatile renewable generations,” *IEEE Trans. Sustain. Energy*, vol. 6, no. 3, pp. 738–747, 2015.

[12] P. J. Vickery, P. F. Skerlj, and L. A. Twisdale, “Simulation of Hurricane Risk in the U.S. Using Empirical Track Model,” *J. Struct. Eng.*, vol. 126, no. 10, pp. 1222–1237, 2000.

[13] “CMA typhoon path data set”, [Online]. Available: https://tcdata.typhoon.org.cn/zjljsjj_sm.html

[14] P. Javanbakht and S. Mohagheghi, “A risk-averse security-constrained optimal power flow for a power grid subject to hurricanes,” *Electr. Power Syst. Res.*, vol. 116, pp. 408–418, 2014.

[15] Y. Wang and D. V. Rosowsky, “Joint distribution model for prediction of hurricane wind speed and size,” *Struct. Saf.*, vol. 35, pp. 40–51, 2012.

[16] R. Darling, “Estimating probabilities of hurricane wind speeds using a large-scale empirical model,” Journal of Climate, vol. 4, no. 10, pp. 1035-1046, 1991.

978-1-6654-0823-3/22/$31.00 ©2022 IEEE